

# **In-situ Growth of well-ordered NiFe-MOF-74 on Ni foam by Fe<sup>2+</sup> Induction as an Efficient and Stable Electrocatalyst for Water Oxidation**

Jiale Xing, Kailu Guo, Zehua Zou, Minmin Cai, Jing Du and Cailing Xu\*

State Key Laboratory of Applied Organic Chemistry, Key Laboratory of Nonferrous Metal Chemistry and Resources Utilization of Gansu Province, Laboratory of Special Function Materials and Structure Design of the Ministry of Education, College of Chemistry and Chemical Engineering, Lanzhou University, Lanzhou 730000, China

C. L. Xu: Tel.: +86-931-891-2589, FAX: +86-931-891-2582, Email: xucl@lzu.edu.cn; xucl921chem@163.com

## **Experimental section**

### **Materials**

Ni foam with a thickness of 1.6 mm and a pore density of 110 ppi was purchased from Changsha Keliyuan. Trisodium citrate, Iron (II) chloride hexahydrate (FeCl<sub>2</sub>·4H<sub>2</sub>O), Nickel(II) nitrate hexahydrate (Ni(NO<sub>3</sub>)<sub>2</sub>·6H<sub>2</sub>O), N, N-dimethylformamide (DMF), ethanol and potassium hydroxide (KOH) were analytical grade and used as received without further purification. 2, 5-dihydroxyterephthalic acid (H<sub>4</sub>DOBDC, 99+%) was obtained from Ningbo polarimetry medical science and Technology Co., Ltd. Nafion was purchased from Sigma-Aldrich. Platinum carbon black (Pt/C, 20%) and iridium (IV) dioxide (IrO<sub>2</sub>) were provided by Alfa Aesar. All aqueous solution used was prepared by the ultrapure water (>18 MΩ cm) prepared by a Millipore system.

## **Preparation of NiFe-MOF-74/NF and Ni-MOF-74/NF**

Firstly, the Ni foam (1 cm × 2 cm) was immersed in an ultrasound bath of acetone, 6 M HCl, DI water and ethanol for 30 min in sequence to activate the surface of Ni foam and then dried at room temperature. Secondly, Trisodium citrate (0.08 mM), FeCl<sub>2</sub>·4H<sub>2</sub>O (0.16 mM), and H<sub>4</sub>DOBDC (250 mg) were dissolved in 7.5 mL DMF-ethanol-H<sub>2</sub>O mixture (1:1:1 (v/v)) under magnetic stirring at room temperature to form a homogeneous solution. Finally, the obtained homogeneous solution and a piece of activated Ni foam (1 cm × 2 cm) were transferred into a vial. And then the vial was put into Teflon-lined stainless-steel autoclave and maintained at 120 °C for 24 h. After cooling to room temperature, the obtained NiFe-MOF-74/NF was washed with ethanol and DMF several times to remove the organic bounds. The final products were then dried at 90 °C for 12 h. For Ni-MOF-74/NF, the similar procedure was employed in the absence of FeCl<sub>2</sub>·4H<sub>2</sub>O and trisodium citrate. To obtain the excellent electrochemical activities of NiFe-MOF-74/NF electrode, the reaction time (12, 24 or 48h) and temperature (120 °C or 150 °C) as well as the dosage of Fe<sup>2+</sup> (0.04 mM, 0.16 mM or 0.32 mM) were optimized. The as-prepared NiFe-MOF-74/NF and Ni-MOF-74/NF were directly used as the working electrode.

## **Material Characterization**

Powder X-ray diffraction (XRD) patterns were obtained by a Rigaku D/M ax-2400 diffractometer with Cu K $\alpha$  irradiation to characterize the crystal structure of the samples. The morphology and microstructure of the samples were investigated by field emission scanning electron microscopy (FESEM, JEOLJSM-S4800) and

transmission electron microscopy (TEM, Tecnai™ G2F30) with energy dispersive spectroscopy (EDX) and selected area electron diffraction (SAED). Infrared spectra were recorded by a Bruker VERTEX 70v FT-IR spectrometer in the range of 500-4000/cm. X-ray photoelectron spectroscopy (XPS) was performed on a PHI-5702 instrument. The Raman spectrum of as-prepared samples was conducted with a LabRAM HR 800 system at 532 nm laser. Inductively coupled plasma-mass spectrometry (ICP-MS) measurements were carried out to determine the concentration of Ni and Fe.

### **Electrochemical Measurement**

All the electrochemical measurements were conducted at room temperature on CHI 760E in 1.0 M KOH. Electrochemical impedance spectroscopy (EIS) was obtained in the frequency range from  $10^5$  to  $10^{-2}$  Hz at a potential of 1.46 V<sub>vs.RHE</sub>. Cyclic voltammetry (CV) was performed at a scan rate of 10 mV s<sup>-1</sup>. The obtained results were adjusted with 95% iR correction to minimize the influence of ohmic resistance. The potentials in this work were converted to a reversible hydrogen electrode (RHE) scale according to the Nernst equation ( $E_{\text{RHE}} = E_{\text{Hg/HgO}} + 0.059 \text{ pH} + 0.197$ ). The overpotential ( $\eta$ ) was calculated according to the following formula:  $\eta \text{ (V)} = E_{\text{RHE}} - 1.23 \text{ V}$ .

### **Preparation of Pt/C and IrO<sub>2</sub> electrode on Ni foam**

The 20wt % Pt/C and IrO<sub>2</sub> (1 mg) were separately suspended in a mixture of deionized water and Nafion (v/v = 200/1) to form a catalyst ink for electrochemistry measurements. The catalyst ink (1 mL) was casted onto Ni foam (1 cm×1 cm) and

dried at room temperature. Catalyst loading on the Ni foam was about  $1 \text{ mg cm}^{-2}$ .

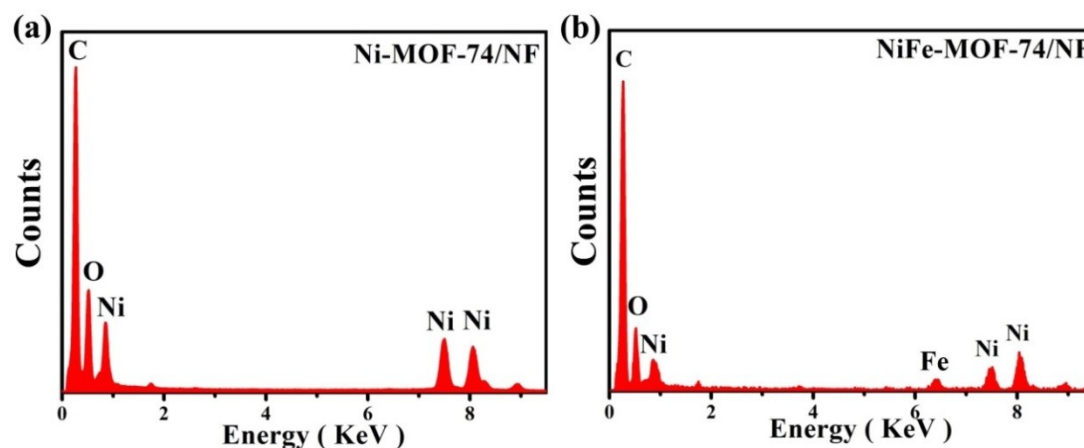


Fig. S1 EDX patterns of (a) Ni-MOF-74/NF and (b) NiFe-MOF-74/NF

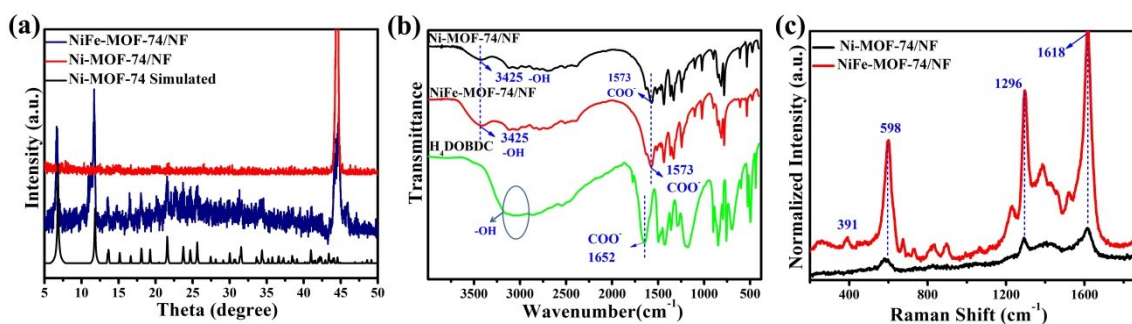


Fig. S2 Simulated data from crystal structure and experimental XRD patterns (a), FTIR (b) and

Raman spectra (c) for Ni-MOF-74/NF and NiFe-MOF-74/NF

For the FTIR of NiFe-MOF-74/NF and Ni-MOF-74/NF in Fig.S2b, the absence of typical absorption peaks related to undissociated hydroxyl and carboxylic acid groups where in the region of  $1600\text{-}3500 \text{ cm}^{-1}$  further reflects that each hydroxyl and carboxylic acid group has been deprotonated in the NiFe-MOF-74 and Ni-MOF-74. This indicates the strong interaction of hydroxyl and carboxylic acid groups in H<sub>4</sub>DOBDC with the Ni<sup>2+</sup> or Fe<sup>2+</sup> ions.<sup>1</sup>

For the Raman spectra of NiFe-MOF-74/NF and Ni-MOF-74/NF in Fig.S2c, The bands at 1618 and 1519 cm<sup>-1</sup> can be associated with the stretching modes of benzene ring.<sup>1, 2</sup> The peak at 1296 cm<sup>-1</sup> can be ascribed to  $\nu(\text{C-O})$  vibration due to the deprotonation of the hydroxyl group.<sup>2, 3</sup> The  $\beta(\text{COO}^-)$  asym vibration is located at 598 cm<sup>-1</sup>. The band at 391 cm<sup>-1</sup> can be attributed to vibrational mode of Ni (Fe)-Oligand.<sup>1-3</sup> In contrast to NiFe-MOF-74, an increase in the full width at half maximum (fwhm) and the reduction in peak intensities were observed for Ni-MOF-74, which was related to the significant structural disorder of Ni-MOF-74.<sup>3, 4</sup>

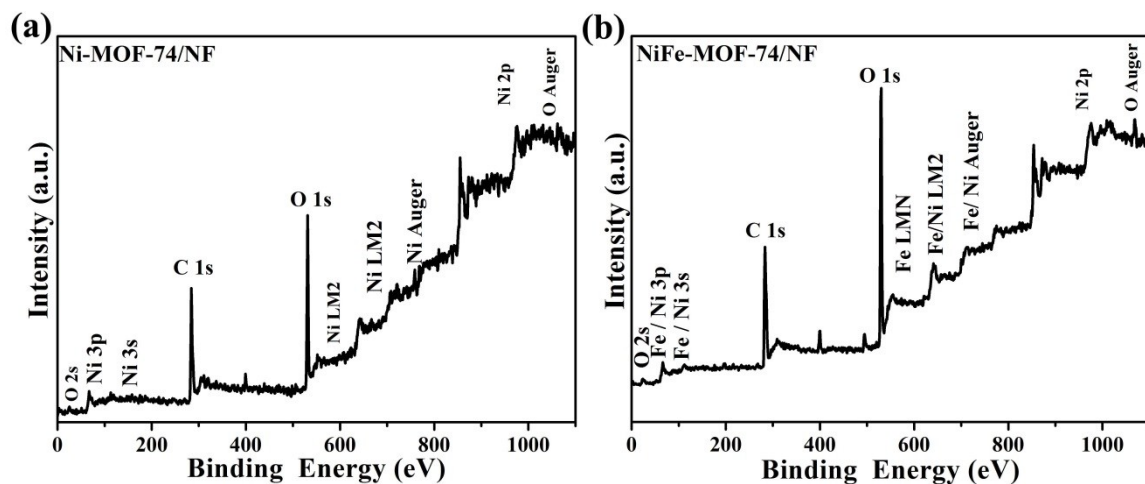


Fig. S3 XPS survey spectra of (a) Ni-MOF-74/NF and (b) NiFe-MOF-74/NF

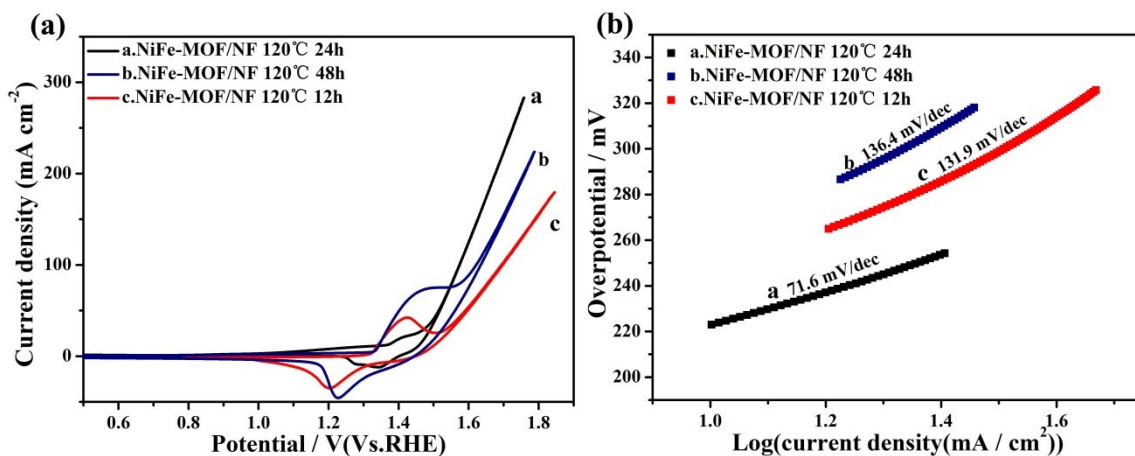


Fig. S4 CV curves (a) and Tafel plots (b) of NiFe-MOF-74/NF reacted at 120 °C with 0.16 mM FeCl<sub>2</sub>·4H<sub>2</sub>O for different time.

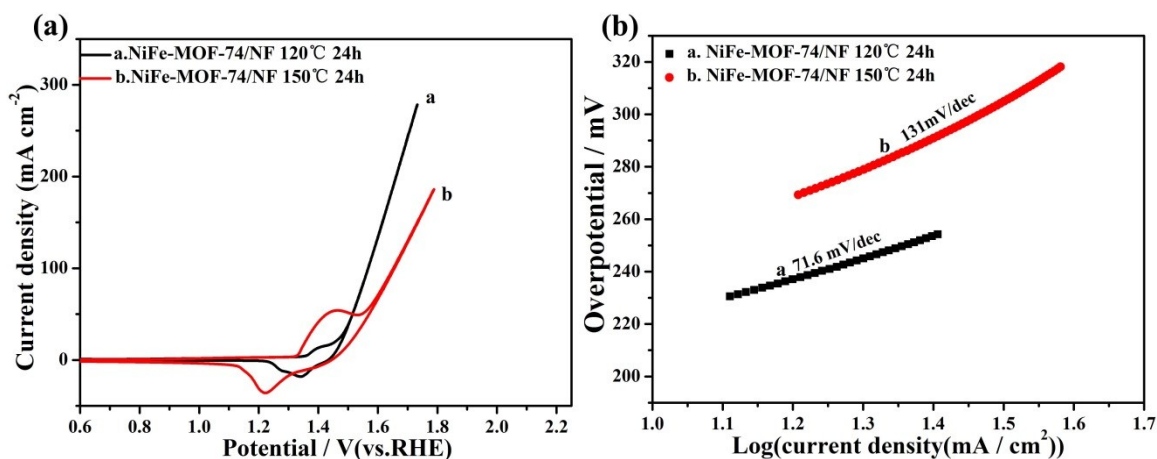


Fig. S5 CV curves (a) and Tafel plots (b) of NiFe-MOF-74/NF reacted under 0.16 mM FeCl<sub>2</sub>·4H<sub>2</sub>O and different temperature for 24h

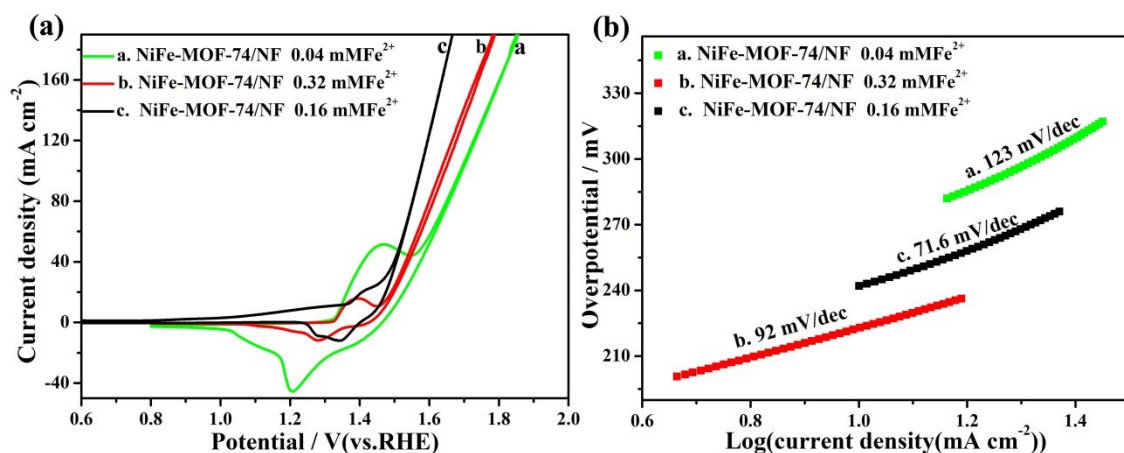


Fig. S6 CV curves (a) and Tafel plots (b) of NiFe-MOF-74/NF reacted under different dosage of  $\text{FeCl}_2 \cdot 4\text{H}_2\text{O}$  at 120 °C for 24h

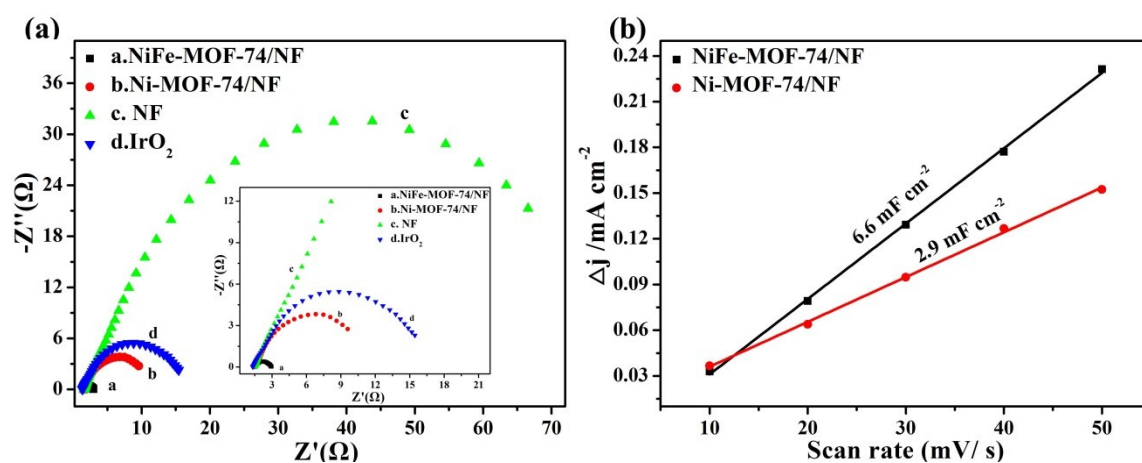


Fig. S7 (a) Electrochemical impedance spectroscopy of Ni-MOF-74/NF, NiFe-MOF-74/NF, Ni foam and  $\text{IrO}_2$  casted onto Ni foam tested at 1.46 V vs. RHE. (b) Difference of current density at 1.0 V (vs. RHE) as a function of the scan rate for Ni-MOF-74/NF and NiFe-MOF-74/NF.

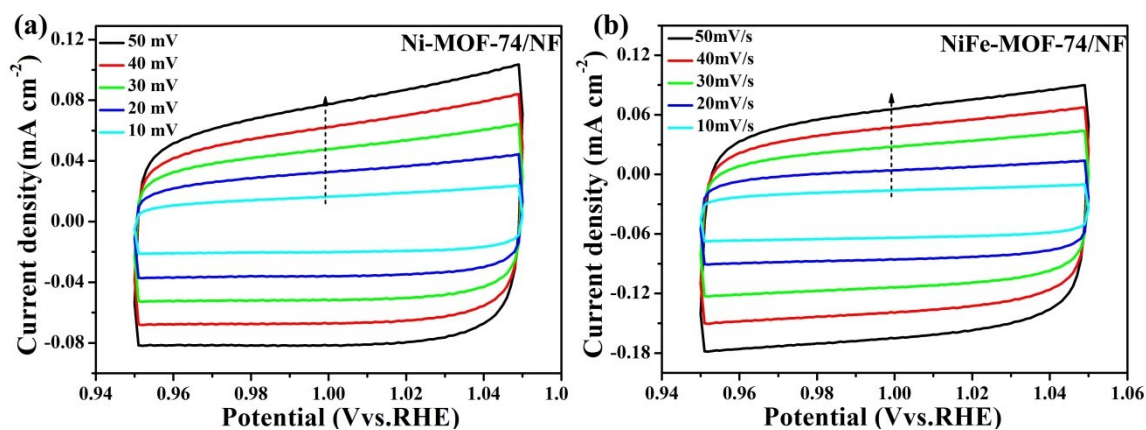


Fig. S8 CV curves at different scan rates in the range of 0.95 and 1.05 V vs. RHE for (a) Ni-MOF-74/NF and (b) NiFe-MOFs-74/NF

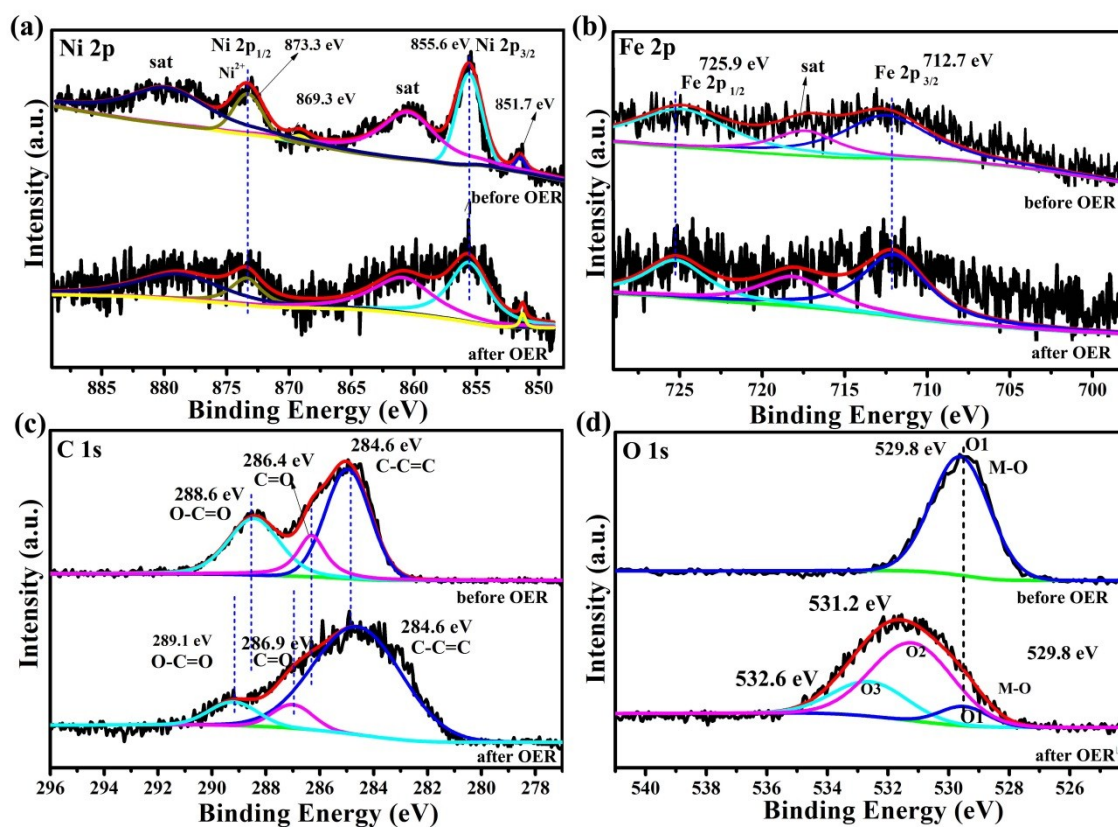


Fig. S9 XPS high-resolution spectra (a-d) of Ni 2p, Fe 2p, C 1s, and O 1s for NiFe-MOF-74/NF before and after 65h chronoamperometric test.

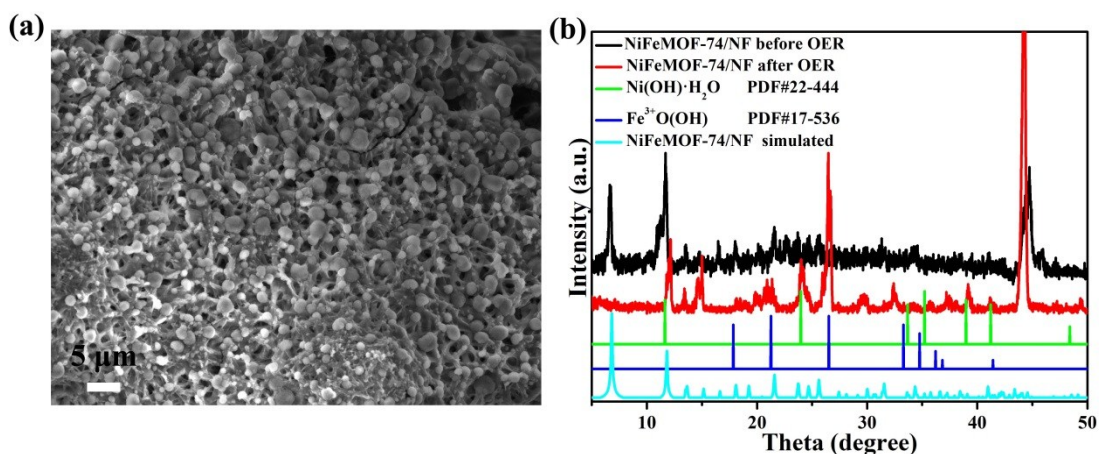


Fig. S10 FESEM images and XRD patterns of NiFe-MOF-74/NF after 65h chronoamperometric test.

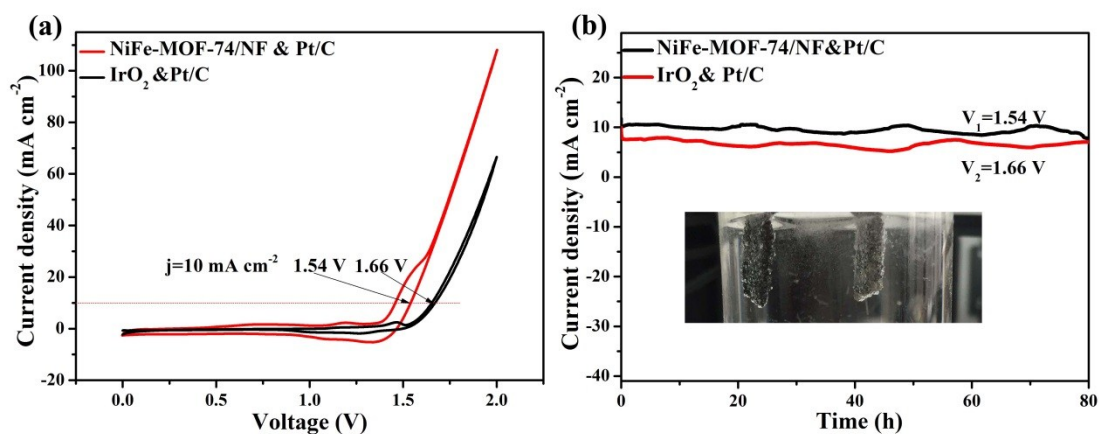


Fig. 11 (a) Cyclic voltammety of NiFe-MOF-74/NF & Pt/C and IrO<sub>2</sub> & Pt/C cell at 10 mV s<sup>-1</sup> and (b) Chronoamperometric curves of NiFe-MOF-74/NF & Pt/C and IrO<sub>2</sub> & Pt/C cell conducted at 1.54 V and 1.66 V, respectively.

Table S1 ICP-AES results of NiFe-MOF-74 microcrystal powders mechanically removed from the

Ni foam

Element	Mass%	Atom%
Ni	25.27	7.33
Fe	1.07	0.33

Table S2 Overpotential and Tafel slope of the reported nonprecious metal electrocatalysts and

MOFs as electrocatalysts for OER (j: current density;  $\eta$ : overpotential at 10 mA cm<sup>-2</sup>)

Catalyst	Electrolyte	$\eta$ (mV)	Tafel Slope (mV/dec)	Reference
CoFe <sub>2</sub> O <sub>4</sub> /C	1 M KOH	240	45	<i>Adv. Mater.</i> 2017, <b>29</b> , 1604437.
NiFe-LDH NPs	1 M KOH	230	50	<i>Chem. Commun.</i> , 2014, <b>50</b> , 6479-6482
NiCo LDH	1 M KOH	367	40	<i>Nano Lett.</i> 2015, <b>15</b> , 1421-1427
MOF NU-1000	1 M KOH	320	59	<i>ACS Appl. Mater. Interfaces</i> , 2015, <b>7</b> , 28223-28230
NiFe LDH/CNT	1 M KOH	240	43	<i>J. Am. Chem. Soc.</i> 2013, <b>135</b> , 8452-8455
FeNi <sub>3</sub> N/NF	1 M KOH	202	40	<i>Chem. Mater.</i> , 2016, <b>28</b> , 6934-6941
NiFe-MOF nanosheets	1 M KOH	240	-	<i>Nat. Commun.</i> 2017, <b>8</b> ,15341-15348
NiFe-UMNs	1 M KOH	260	30	<i>Nano energy</i> 2018, <b>44</b> , 345-352
CUMSs-ZIF-67	1 M KOH	320	185	<i>Nano energy</i> 2017, <b>41</b> , 417-425
CoFeP <sub>x</sub>	1 M KOH	244	58	<i>ACS Appl. Mater. Interfaces</i> , 2017, <b>9</b> , 362-370
Fe/Ni-BTC@NF	1 M KOH	270	47	<i>ACS Appl. Mater. Interfaces</i> 2016, <b>8</b> , 16736-16743
Cu-MOF	0.5 M H <sub>2</sub> SO <sub>4</sub>	310	89	<i>Adv. Funct. Mater.</i> 2013, <b>23</b> , 5363-5372
hy-Co <sup>2+</sup> /Fe <sup>3+</sup>	1 M KOH	265	37	<i>J. Mater. Chem. A</i> , 2018, <b>6</b> , 805-810
UTSA-16	1 M KOH	408	77	<i>ACS Appl. Mater. Interfaces</i> , 2017, <b>9</b> , 7193-7201
NiCo - POM/Ni	1M KOH	360	126	<i>Angew. Chem.</i> 2017, <b>56</b> , 4941-4944
NiCo-UMOFNs	1M KOH	189	42	<i>Nature Energy</i> , 2016, <b>1</b> , 16184
CoOx-ZIF/C	1M KOH	318	70	<i>Adv. Funct. Mater.</i> 2017, <b>27</b> , 1702546
MAF-X27-OH(Cu)	1M KOH	292	-	<i>J. Am. Chem. Soc.</i> 2016, <b>138</b> , 8336-8339
NiCo - POM/Ni	1M KOH	360	126	<i>Angew. Chem.</i> 2017, <b>56</b> , 4941-4944
<b>NiFe-MOF-74</b>	<b>1 M KOH</b>	<b>223</b>	<b>76</b>	<b>This work</b>

Notes and references

- 1 K. Tan, S. Zuluaga, Q. Gong, P. Canepa, H. Wang, J. Li, Y. J. Chabal and T. Thonhauser, *Chem. Mater.*, 2014, **26**, 6886-6895.
- 2 G.H. Albuquerque, R.C. Fitzmorris, M. Ahmadi, N. Wannemacher, P.K. Thallapally, B.P. McGrail and G.S. Herman, *Cryst. Eng. Commun.* 2015, **17**, 5502-5510.
- 3 V. K. LaMer and R. H. Dinegar, *J. Am. Chem. Soc.*, 1950, **72**, 4847-4854.
- 4 F. Bonino, S. Chavan, J. G. Vitillo, E. Groppo, G. Agostini, C. Lamberti, Pa. D. C. Dietzel, C. Prestipino and S. Bordiga, *Chem. Mater.* 2008, **20**, 4957-4968.